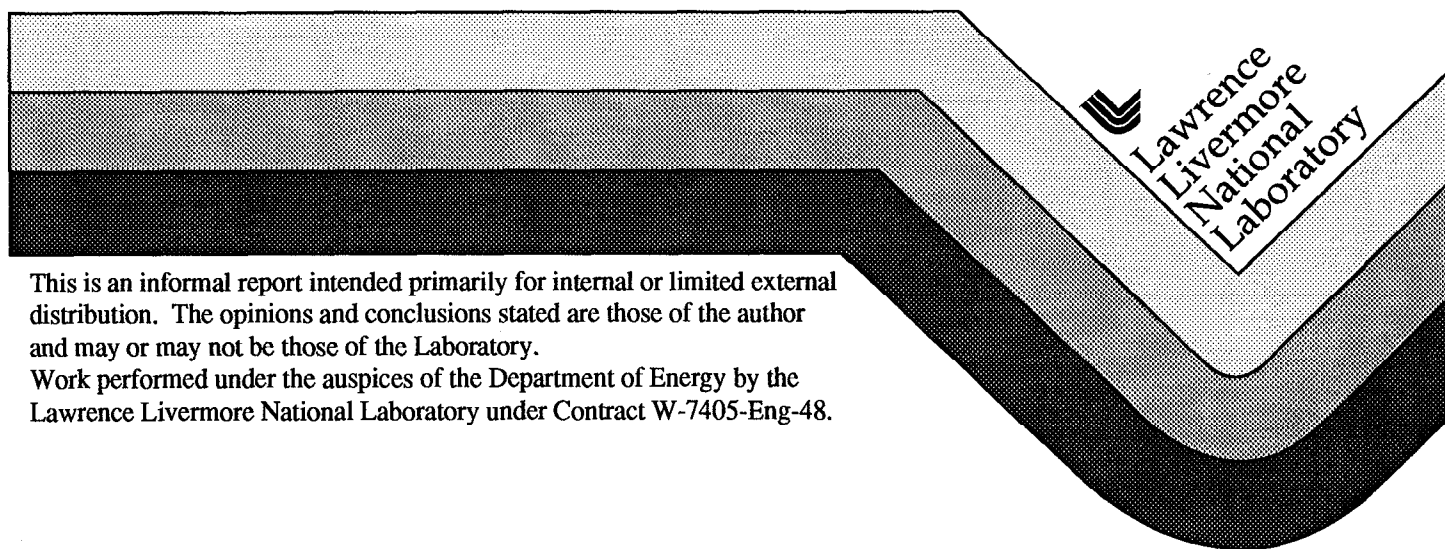


# The $^{239}\text{Pu}(n,2n)^{238}\text{Pu}$ Cross Section: Preliminary Calculations

M. Alan Ross  
H. Chen  
G. Reffo  
R. M. White

March 12, 1999



#### DISCLAIMER

This document was prepared as an account of work sponsored by an agency of the United States Government. Neither the United States Government nor the University of California nor any of their employees, makes any warranty, express or implied, or assumes any legal liability or responsibility for the accuracy, completeness, or usefulness of any information, apparatus, product, or process disclosed, or represents that its use would not infringe privately owned rights. Reference herein to any specific commercial product, process, or service by trade name, trademark, manufacturer, or otherwise, does not necessarily constitute or imply its endorsement, recommendation, or favoring by the United States Government or the University of California. The views and opinions of authors expressed herein do not necessarily state or reflect those of the United States Government or the University of California, and shall not be used for advertising or product endorsement purposes.

This report has been reproduced  
directly from the best available copy.

Available to DOE and DOE contractors from the  
Office of Scientific and Technical Information  
P.O. Box 62, Oak Ridge, TN 37831  
Prices available from (615) 576-8401, FTS 626-8401

Available to the public from the  
National Technical Information Service  
U.S. Department of Commerce  
5285 Port Royal Rd.,  
Springfield, VA 22161

# The $^{239}\text{Pu}(n,2n)^{238}\text{Pu}$ Cross Section: Preliminary Calculations

M. Alan Ross, H. Chen, G. Reffo and R. M. White

## ABSTRACT

The primary motivation for the present work is to provide theoretical values for the ratio of the partial  $^{239}\text{Pu}(n,2n\gamma)^{238}\text{Pu}$  to total  $^{239}\text{Pu}(n,2n)^{238}\text{Pu}$  cross section for several discrete gamma transitions. Results and conclusions of preliminary calculations from threshold to 20 MeV are presented. Calculations are based on theoretical models with parameters obtained from the literature or from our *ad hoc* systematics. Optical model cross sections and transmission coefficients were determined using the coupled-channels method. The calculations included a preequilibrium component followed by multiple particle and gamma-ray emissions. Fission competition was included at all stages of de-excitation. Suggestions for further verifications and possible improvements are provided.

## 1. INTRODUCTION

It is understood that the (n,2n) cross section in the actinide region is relevant to radiochemical diagnostics. Experimental measurements of the (n,2n) cross section are complicated by the presence of neutron emissions following the fission process. There is currently a significant experimental effort in N-Division to provide information necessary to the determination of the (n,2n) cross section by measuring the population probability of discrete levels via gamma transitions between levels in the residual nucleus after the (n,2n) reaction. Gamma transitions between the discrete levels  $8^+ \rightarrow 6^+$ ,  $6^+ \rightarrow 4^+$ , and  $4^+ \rightarrow 2^+$  in  $^{238}\text{Pu}$  are currently being measured using the GEANIE spectrometer [1]. These measurements, however, can provide only partial (n,2n) cross sections. Nuclear theory and modeling calculations are required for the complete description of the (n,2n) reaction. We have initiated a detailed theoretical study of the (n,2n) process in the actinide region, with particular attention to gamma-ray de-excitation. This study requires a correct interpretation of a large number of cross sections, *e.g.*, total, elastic, inelastic, fission, (n,xn), as well as contributions from various reaction mechanisms (direct, precompound and compound nucleus) and from different emission competitions (particle, gamma, fission). The modular system of codes IDA [2] has been used for the present calculations. It should be stressed that such theoretical study and comparisons with experimental data constitute a new and important test for the theoretical tools currently available. Accordingly, we have used and tested our models and

codes with the experimental (n,2nxy) cross sections presently available and have directed our efforts towards increasing the accuracy in plutonium cross sections calculations in anticipation of the results from the GEANIE spectrometer.

## 2. MODELS AND CODES ADOPTED

### 2.1 Particle Channels

**Optical model and direct collective inelastic scattering.** The highly deformed target in study here,  $^{239}\text{Pu}$ , requires the use of coupled-channel calculations for a more proper account of the optical model cross sections and, in particular, of the direct neutron inelastic scattering. For this purpose the generalized optical model code ECIS [3] has been coupled to the IDA system to run in tandem with the module PENELOPE for Hauser-Feshbach plus exciton model calculations. Thus ECIS provides total, shape elastic and transmission coefficients in the neutron channels outgoing from compound nucleus. PENELOPE allows for multiple particle and gamma ray cascading emissions using quantities (*e.g.*, cross sections and transmission coefficients) calculated by ECIS, under the condition of flux conservation.

Two sets of optical model parameters were used to test the sensitivity of the calculations to the optical model parameterization. One set was from Madland and Young [4], which was deduced from an analysis of neutron scattering experiments in the actinides up to 10 MeV. The second set of optical parameters was from Dietrich [5] and provides total cross section calculations from 10 keV to 30 MeV.

**Preequilibrium contributions.** The preequilibrium reaction mechanism was treated assuming the one-gas exciton model option in PENELOPE, with spin and parity conservation [6], and using the very well known Williams quasi-particle level density. The effect of nucleon-nucleon interactions in the presence of a mean field was taken into account in terms of the Fermi motion of nucleons. Reflections and refractions at the nuclear surface were also included [7]. Preequilibrium contributions are dominated by the quasi-particle level density, being rather insensitive to other refinements in the treatment of the internal transitions [8]. Preequilibrium dominates the first neutron emission above 12 MeV, however, no contribution from multiple preequilibrium emission was found. In particular, compound nucleus cascade emissions following preequilibrium emission

were found to be quite important. In the present preliminary calculations, preequilibrium capture and preequilibrium proton emissions were neglected.

**Compound nucleus emissions.** The treatment of compound nucleus formation and decay follows the well-known Hauser-Feshbach formalism with energy, spin and parity conservation. The proviso in the coupled-channel optical model approximation is that the transmission coefficients also depend on total spin and parity:  $T_{lj}^{J\pi}(E)$ .

## 2.2 Gamma Channels

Gamma decays are calculated according to the Brink-Axel approach. Inverse photon absorption cross sections were approximated with Lorentzian forms [9]. E1, M1, and E2 transitions have been allowed. The giant resonance parameters systematics for the split E1 giant resonance from Ref. 9 provide photon absorption cross section to within a few percent. The well known dependence of the gamma decay widths on spin and parity selection rules and on the ratio of final to initial level density play an important role in calculations of gamma spectra and discrete level population probabilities. This has required, therefore, special effort in the analysis of nuclear structure details, and is discussed in the following section. We stress that whenever experimental data were available for total radiative widths of neutron resonances, tests have been performed in the gamma channel to verify proper level density parameterizations. These tests include the comparison of the distribution of the experimental total radiative widths with the calculated  $\chi^2$  distribution and its respective degrees of freedom.

## 2.3 Fission channel

Fission competition has been allowed in all compound nucleus decays including those following preequilibrium emissions. The model adopted is the that of Bjornholm-Lynn [10]. The model assumes double-humped fission barriers where the transmission coefficients are determined using the Hill-Wheeler inverted parabola approach. Level densities above the fission barriers are assumed to have a constant temperature behavior. The Bjornholm-Lynn reference contains values for the fission barriers and level density parameters for all Pu isotopes needed for the present calculation.

### 3. NUCLEAR STRUCTURE

Nuclear structure properties are involved in all channels in terms of nuclear deformation and excitation modes available. In particular, the level density plays a determinant role in its capability to describe energy, spin, and parity distributions of nuclear configurations populated at higher energies. The spectroscopy of low-lying levels becomes important in describing tails of emission spectra. Experimental gamma branchings of discrete levels ensure the proper termination of the gamma cascades following the decay of excited nuclei. In order to ensure a realistic description of the relevant nuclear structure, a very accurate procedure has been used and is described below.

Currently, most available level density approaches are unable to reproduce the level spacing,  $D$ , because they are based on the Fermi gas model, which is applicable only when the nucleon correlations can be ignored. Also, the statistical considerations in the Fermi gas model apply only when the classes of nuclear levels characterized by  $(E, J, \pi)$  constitute large ensembles. As both fundamental assumptions do not apply at low excitation energies, it is obvious that such approaches can constitute only guidelines. Absolute values of parameters are to be adjusted using experimental information. The spacing of neutron resonances,  $D$ , has been used to renormalize the value of the level density at the neutron binding energy, which in turn is used to fix level density parameters. The starting point of our investigation was, therefore, a statistical analysis of neutron resonances based on several tests available in IDA. These include, staircase analysis of neutron resonance energies and neutron reduced widths, and a number of other statistical tests using the integrated Porter-Thomas distribution (full distribution, missing level estimator, truncated distribution and segmented distribution). After a few iterations, an accurate statement can be made of the quality of the resonance parameter sample along with estimates of average neutron resonance parameters and their respective uncertainties. The two-formulae level density approach currently used in IDA is the one of Gilbert and Cameron described in [9]. The high energy formula is renormalized to reproduce the density of neutron resonances, the low energy formula is renormalized to reproduce discrete level energy, spin and parity distributions with matching conditions being imposed on the functions describing the two regions. This procedure ensures reliable level density treatment for excitation energies up to and beyond the neutron separation energy.

The Gilbert and Cameron formalism completely relies on two parameters, the nuclear temperature and the density of single particle states around the Fermi level,  $T$  and  $a$ , respectively. Using the shell model as guidance and following the precise physical meanings of  $T$  and  $a$ , we have derived quite reliable local systematics. These systematics have been used for those nuclei where no experimental data are available. The uncertainties in the parameters used in the level density formalism are due to: 1) the experimental errors in the level spacing,  $D$ , 2) errors in the discrete levels (mainly missing levels) and 3) errors involved in the model approximations. These uncertainties are accounted for in the estimate of the errors associated with our model calculations of cross sections.

#### 4. SENSITIVITY STUDIES AND ERROR ANALYSIS

The primary motivation for the present calculations is to provide theoretical values for the ratio of the partial  $(n,2n\gamma)$  to total  $(n,2n)$  cross section for several discrete gamma transitions. In order to assign an estimate of the uncertainty in this ratio, several additional calculations were performed under extreme assumptions. These calculations included: suppression of the preequilibrium component, use of two different level density schemes in the preequilibrium process, suppression of fission competition, use of a spherical optical potential, doubling of the spin cutoff factor  $\sigma^2$  in  $^{238}\text{Pu}$  to determine the effects of missing high-spin levels, and finally, adding a hypothetical collective rotational band in  $^{238}\text{Pu}$ . For the present calculations, uncertainties in the total level density have been determined to be negligibly small for the residual nuclei involved. Results of these sensitivity studies are summarized in the next section.

#### 5. RESULTS AND DISCUSSION

The relevant cross sections involved in the calculation of the  $(n,2n)$  cross section are numerous and not all of them can be compared with experiment. The total incoming flux is shared among different reaction mechanisms and among different reaction channels. Optical model parameterization determines the sharing of total cross section between shape elastic and reaction cross sections. An overestimate of the shape elastic cross section reduces the size of reaction cross section and of all the further sharing in the various absorption channels. Similarly, an overestimate of any dominant decay channel of the compound nucleus reduces the size of all others. The sharing of the incoming flux is dealt with by treating the different mechanisms involved sequentially.

In our calculations, we first considered the impact of optical model parameterization in the sharing of the total cross section between shape elastic and absorption. The two different sets of optical model parameters were chosen, [4], and [5], are considered to be reliable in a wide energy interval. These parameterizations, however, gave sizeably different results, thus providing indications about the uncertainties propagated from the optical model to our (n,2n) calculations. In Fig. 1, total cross sections are shown for the two optical potential parameter sets along with evaluated experimental data. The data are better reproduced with the parameterization of ref. [5], being within  $\pm 1\%$  over the entire energy region. Calculations of  $\sigma_{\text{tot}}$  using parameters from ref. [4] are within  $\pm 5\%$  of the experimental data. Experimental information on elastic scattering is very sparse in this energy region, angular distributions at 5, 5.5 and 14.1 MeV were considered, see Figs. 2, 3, 4. The calculated angular distributions do seem to reproduce the experimental data although it is difficult to be quantitative since most of the elastic cross section is at small angles where there is little or no experimental data.

The calculated fission cross sections are within 10% of a new evaluation of the experimental data with the optical model parameterization [4] being systematically low, and with parameterization [5] being systematically high above 8 MeV, as shown in Fig. 5. The only difference between our two curves is in the different optical model parameter variations chosen, fission barriers and fission level density parameters are the same. If we assume that the two optical model parameter sets are quite reasonable when compared to total cross and shape elastic cross section, this result illustrates how the uncertainties in the optical model quantities may influence the fission cross section and all other reaction cross sections.

The calculated (n,2n) cross sections show a similar behavior, results from set [5] being higher than those from [4], see Fig. 6. A third calculation of the (n,2n) cross section is shown in Fig. 6. For this curve a different level density option for the preequilibrium process was chosen, by reparameterizing the Williams formula to be consistent with the total level density. For completeness, previous theoretical evaluations from ENDF/B-VI [11] and Blann and White [12] are also shown in Fig. 6. It is evident that there are large discrepancies among calculations and between calculations and experimental data. Both our (n,2n) calculations and those of Blann and White are substantially lower than ENDF/B-VI. Careful consideration of the experimental data for total, elastic,



fission and with the limited amount of reaction cross section data would seem to indicate that the available  $(n,2n)$  cross section data are too high. This is further supported by the fact that  $(n,n')$  and  $(n,3n)$  (when energetically possible) are also competing with the  $(n,2n)$  process in the energy of interest for the present calculations.

Gamma ray cascades  $(n,2nx\gamma)$ , following the  $n,2n$  process, have been calculated. Up to 7 sequential gamma decays have been allowed. The cascades ending in the ground state have been distinguished from those ending in the  $8^+$  level at 0.513 MeV, the  $6^+$  level at 0.303 MeV, and the  $4^+$  level at 0.146 MeV. The ratios of the gamma cascade cross section ending at the specified level to the total gamma cascade cross section are shown in Fig. 7 for two calculations: IDA using [4] and IDA using [5].

Results of the gamma cascade ratio for the  $6^+$  state are shown in Fig. 8. There is a slight sensitivity to the size of the fission channel. The ratio without fission competition is 15% higher above 14 MeV. The results obtained using a spherical optical potential and increasing the spin distribution did not have a large effect on the ratio. The ratio was also not sensitive to two preequilibrium level density schemes available in IDA. It should be stressed, however, that as the energy increases the results become more sensitive to the fraction of preequilibrium contributions because the spin distributions of the residual nucleus after a preequilibrium emission is more peaked towards lower values. Preequilibrium is obviously important in these calculations, the ratio increases by 50% above 14 MeV if it is neglected completely. Finally, the ratio is not sensitive to the possible loss of a collective rotational band in  $^{238}\text{Pu}$ . Calculations of the  $6^+$  ratio were made assuming the level scheme of  $^{238}\text{Pu}$  had an additional band head starting with a  $2^+$  state at 0.725 MeV, continuing up to a  $7^+$  state at 1.147 MeV. The result was a 4% decrease in the calculated  $6^+$  ratio.

With the exception of no fission and no preequilibrium, it appears that the ratios considered are quite stable with respect to variations of the parameters used in the calculations. This is probably due to a partial error cancellation in the ratio.

## 6. SUGGESTIONS AND CONCLUSIONS

We have seen that the  $(n,2n)$  process, in a large fraction of the energy interval of interest here, represents a dominant or at least a sizeable competition with respect to other reaction channels. This allows us to restrict our concerns about error propagation only to uncertainties coming from dominant competitions. This consideration immediately reduces the field of investigation to errors propagated from the optical model, the fission channel, preequilibrium and level densities. The calculations shown in Fig. 6 (solid, long-dashed curve and dot-dash curves) provide an estimate of the uncertainty in the  $(n,2n)$  cross section at the present time, and clearly indicate the importance of the optical model, fission channel, and preequilibrium. Calculations using Dietrich's parameterization give a very good fit to the total cross section. There is still room, however, to verify if any improvement can be gained by a global fit including also more specific information on elastic and nonelastic data. The experimental fission cross section is known in the 5-25 MeV energy region to better than  $\pm 2\%$ . One easy improvement would be to use this information to fix the parameters describing the fission channel (namely fission level density parameters and the fission barriers) to match the experimental cross section values.

As far as the gamma cascade ratios are concerned, one has to note that those following preequilibrium emissions take place between levels of spin generally lower than the spin involved in the cascades following compound emissions. Therefore, the relative size of preequilibrium and compound contributions are expected somehow to influence the ratios of concern here. A thorough study of this aspect is necessary. In particular, one element of uncertainty could be the commonly adopted Williams formula for quasi-particle level densities. The effect of microscopic combinatorial calculations on the fraction of preequilibrium contributions may be relevant to the purpose. These level densities are more precise and tend to reduce preequilibrium contributions. Finally, in preequilibrium emission, it is quite possible that most of the available energy is picked up by a recoil proton which may exceed the coulomb barrier, therefore inclusion of proton emission might also contribute to further reduce preequilibrium neutron emissions.

An analysis of the spin distribution of low-lying levels in  $^{238}\text{Pu}$  shows a considerable loss of high spin levels. Another minor improvement could be to take into account all missing rotational levels so that the spin distribution takes its proper form and then use these discrete level schemes and the corresponding spin cutoff factor.

## ACKNOWLEDGMENTS

The authors would like to thank Frank Dietrich, Marshall Blann and Lee Bernstein for their frequent and useful discussions during the preparation of this manuscript.

## REFERENCES

1. L. Bernstein, LLNL, private comm.
2. G. Reffo and F. Fabbri, unpublished.
3. J. Raynal, code ECIS95, unpublished
4. D. G. Madland and P. G. Young, *Neutron-Nucleus Optical Potential for the Actinide Region*, International Conference on Neutron Physics and Neutron Data for Reactors and Other Applied Purpose, September 25-29, 1978, United Kingdom.
5. F. Dietrich, LLNL, private comm.
6. J.M. Akkermans, H. Gruppelaar, and G. Reffo, Phys. Rev. C **22** 737(1980).
7. G. Reffo, and C. Costa, Int. Conf. On Nuclear Physics, Florence Aug. 29-Sept 3, 1983, Vol. 1, pg 85, 1983, P. Blasi and R.A. Ricci, Editors, Publisher Tipografia Compositori, Bologna, Italy.
8. H. Herman and G. Reffo, Lectures for the International Workshop on Nuclear Reaction Data and Nuclear Reactors, Trieste 15 April - 17 May 1996, A Gandini and G. Reffo editors, Vol. 1, pg. 115, World Scientific, 1998.
9. G. Reffo, *Parameter Systematics for statistical theory calculations of neutron reaction cross sections*, IAEA(UNESCO) Winter Courses in Nuclear Physics and Reactors, Trieste, January 17- March 10, 1978 published by IAEA as IAEA-SMR-43 1980. CNEN report RT/FI(78)11, 1978.
10. S. E. Bjornholm and J. E. Lynn, *The Double-Humped Fission Barrier*, Rev. of Mod. Phys. **52** 725(1980)
11. P. Rose, EDF-201: ENDF/B Summary Documentation, 4th Edition (ENDF/B-VI), Brookhaven National Laboratory report BNL-NCS-17541 [ENDF-201] (1992).
12. M. Blann and R. M. White, *Nuclear Modeling of the  $^{239}\text{Pu}(n,xn)$  Excitation Function*, Lawrence Livermore National Laboratory Report, UCRL-19980 (1984).

Work performed under the auspices  
of the U.S. Department of Energy by  
Lawrence Livermore National Laboratory  
under Contract W-7405-ENG-48.

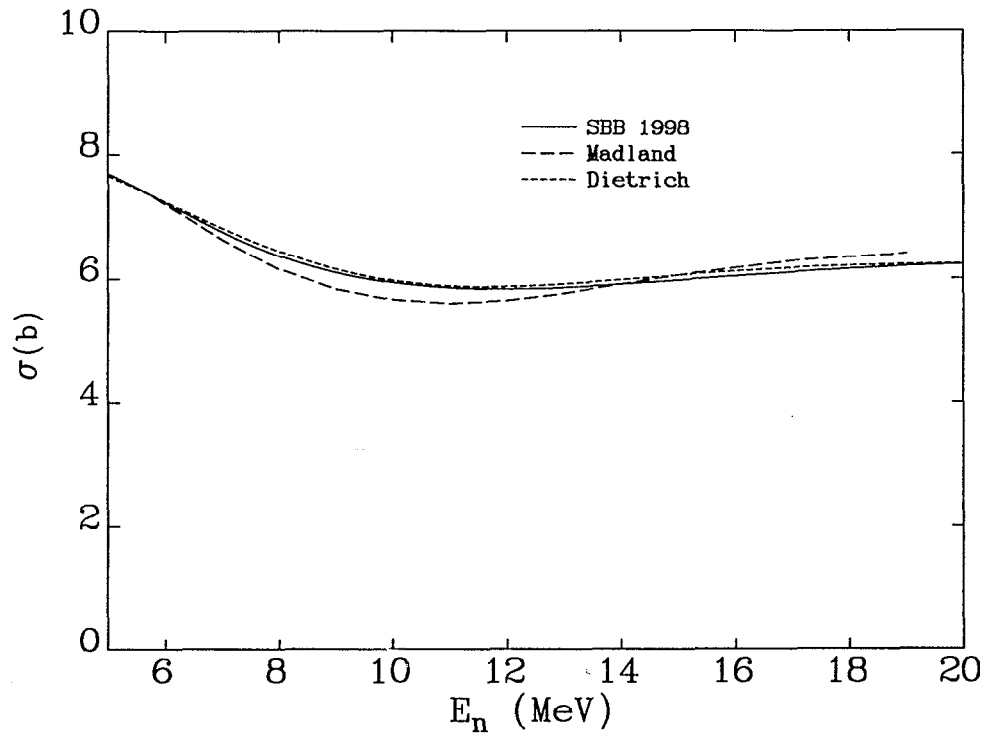


Fig. 1. Cross section for  $^{239}\text{Pu}(n,\text{tot})$ . SBB is the LLNL Stewardship Barn Book evaluation.

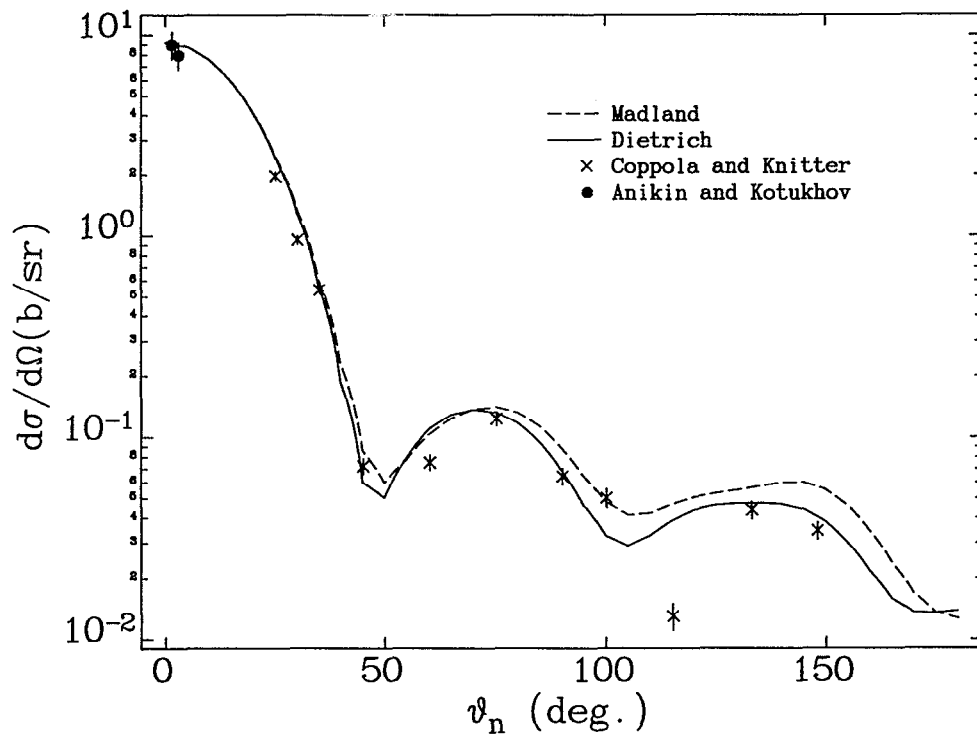


Fig. 2. Angular distribution for  $^{239}\text{Pu}(n,\text{el})$  at 5.0 MeV.

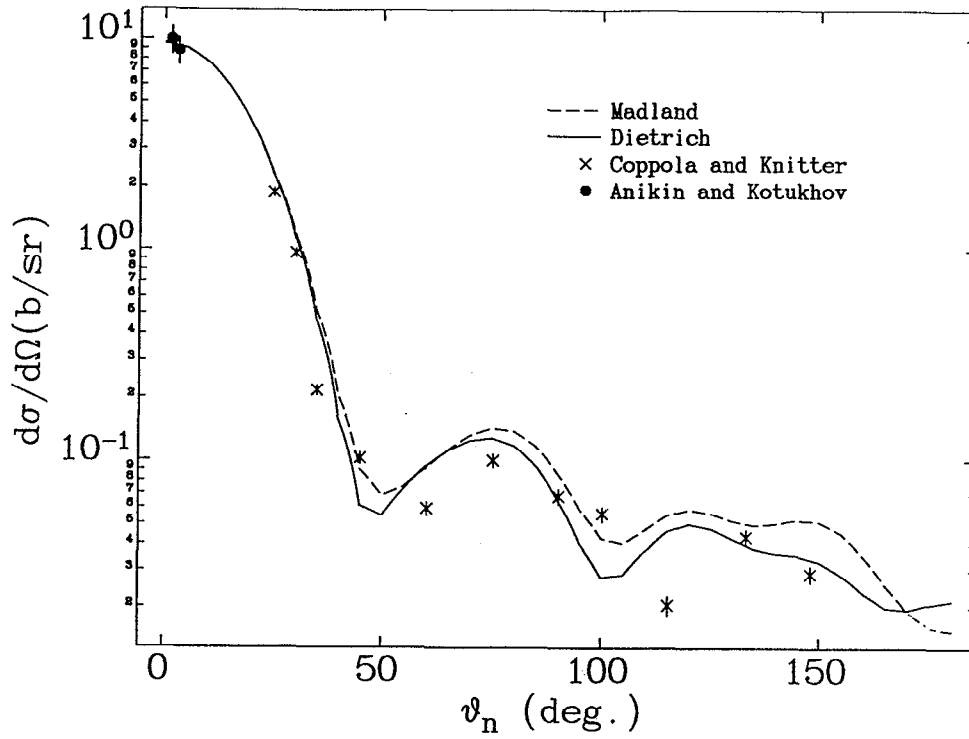


Fig. 3. Angular distribution for  $^{239}\text{Pu}(n,\text{el})$  at 5.5 MeV.

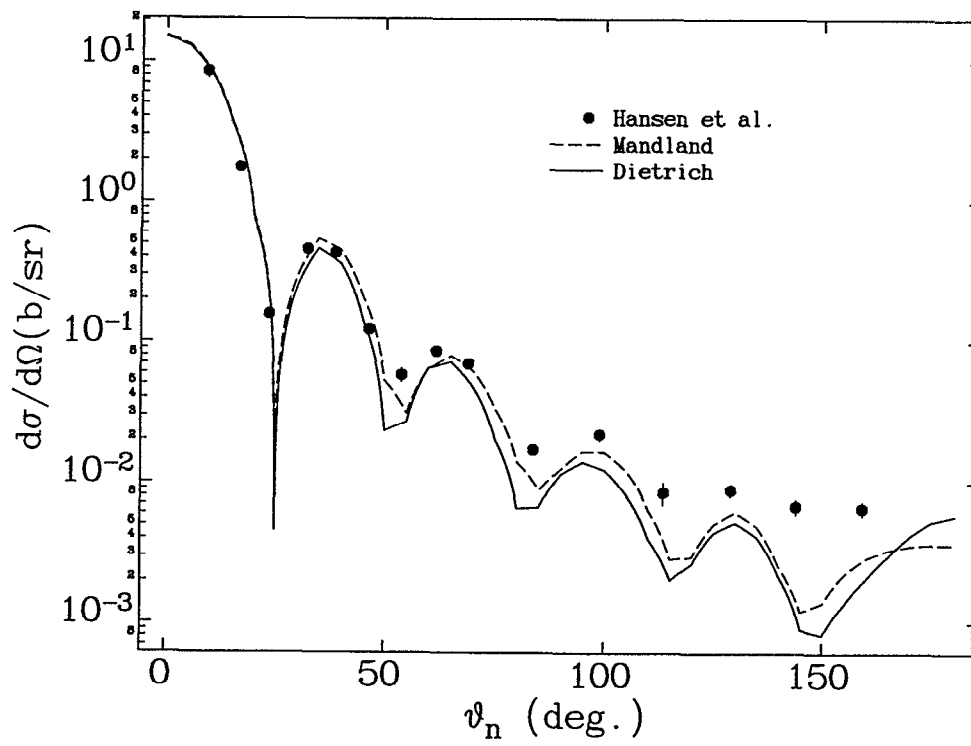


Fig. 4. Angular distribution for  $^{239}\text{Pu}(n,\text{el})$  at 14.1 MeV.

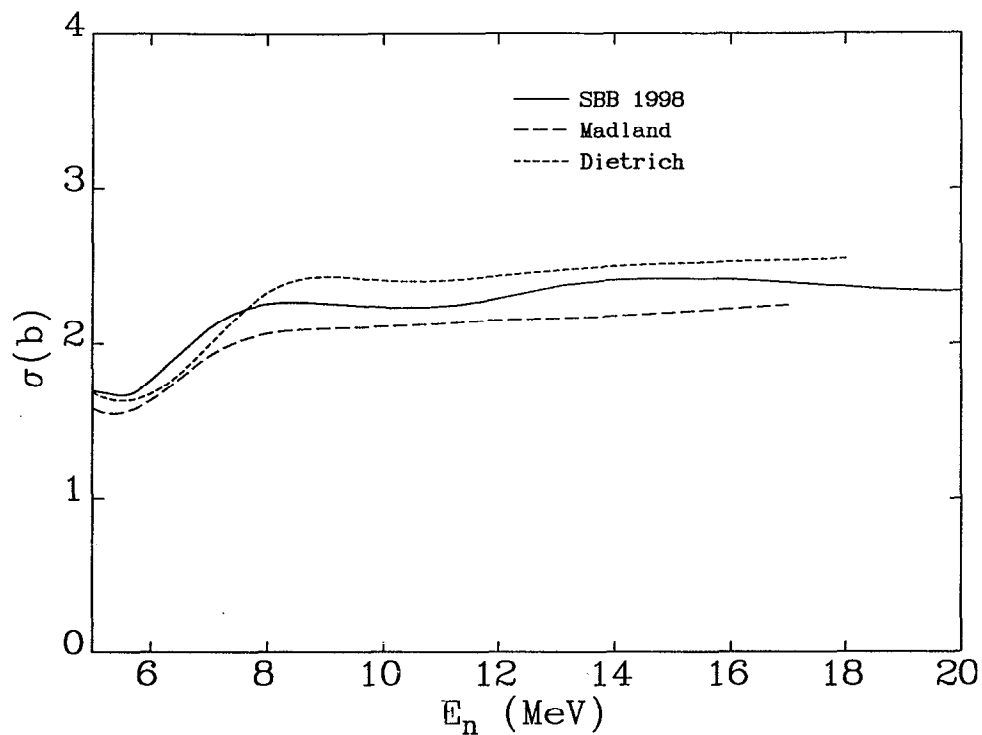


Fig. 5. Cross section for  $^{239}\text{Pu}(n,f)$ . SBB is the LLNL Stewardship Barn Book evaluation.

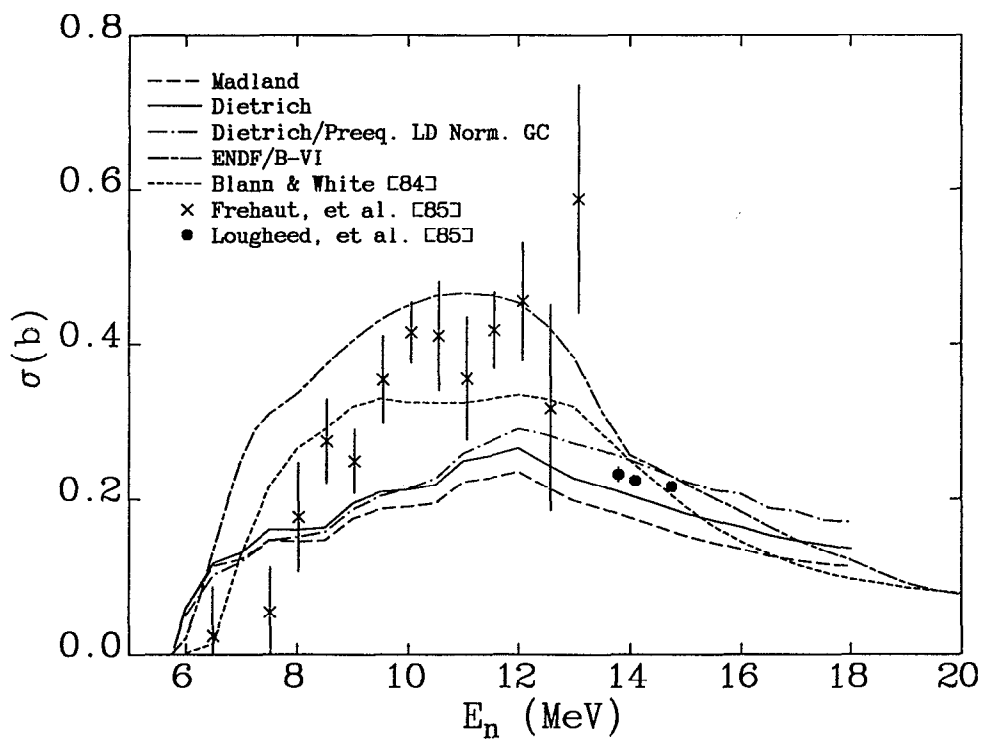


Fig. 6. Cross section for  $^{239}\text{Pu}(n,2n)^{238}\text{Pu}$ .

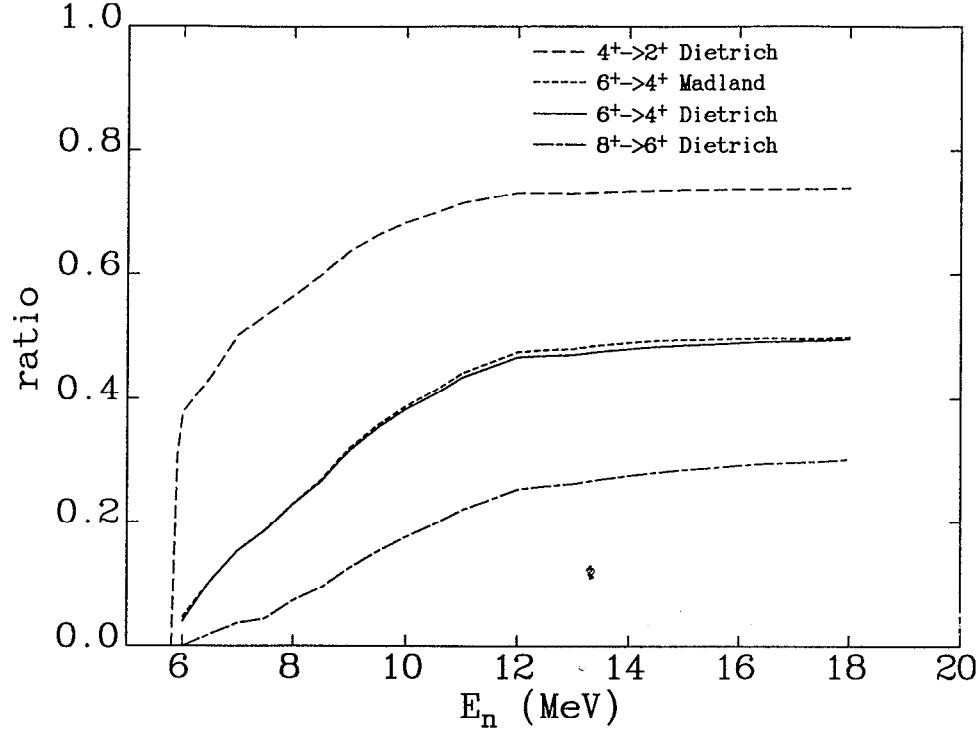
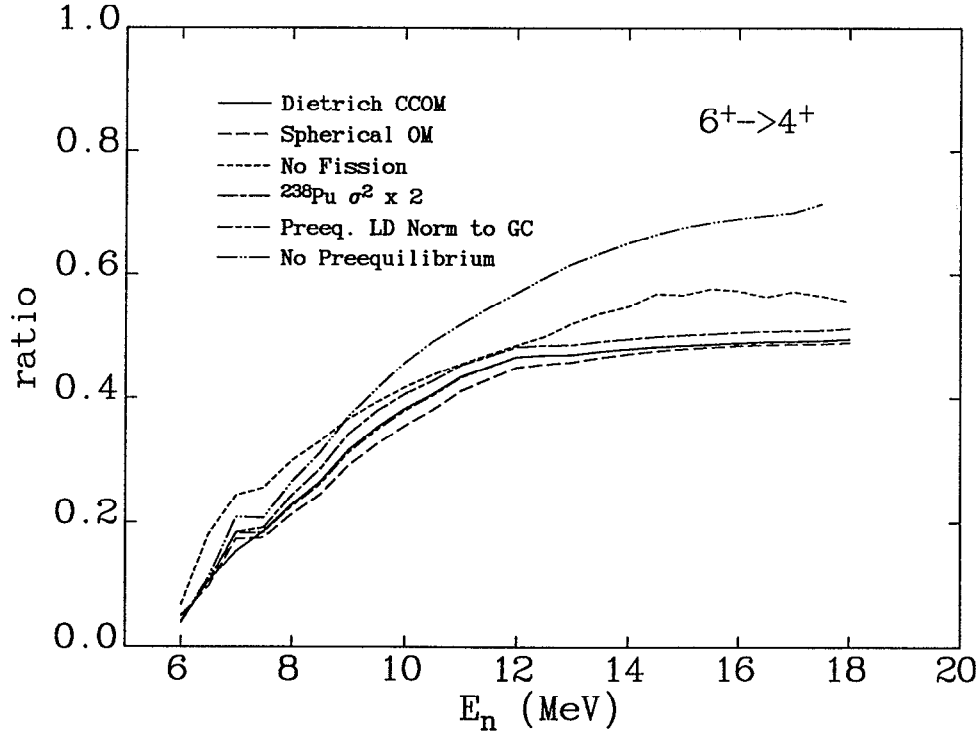


Fig 7. Ratio of  $^{239}\text{Pu}(n,2n)^{238}\text{Pu}/^{239}\text{Pu}(n,2n)^{238}\text{Pu}$  cross section for the  $8^+$ ,  $6^+$ ,  $4^+$  states in  $^{238}\text{Pu}$ .



8. Sensitivity study of the  $6^+$  to total cross section ratio for  $^{239}\text{Pu}(n,2n)^{238}\text{Pu}/^{239}\text{Pu}(n,2n)^{238}\text{Pu}$ .